Subparticle stress fields in granular solids

Vincent Topin, Farhang Radjai, and Jean-Yves Delenne
LMGC, CNRS-Université Montpellier 2, UMR 5508, Pl. E. Bataillon, 34095 Montpellier Cedex 5, France
(Received 16 February 2009; published 7 May 2009)

We rely on the lattice element method to simulate and analyze the stress fields at subparticle scales in two-dimensional granular solids composed of particles of variable stiffness together with an interstitial matrix of variable volume fraction. We find that the contact force distributions as approached from the subscale stresses are similar to those obtained from a particle-scale discrete element approach. This means that the well-known properties of force distributions in model granular media, with hard particles and without an interstitial phase, can be extended to materials such as concrete and sandstone involving a jammed particle phase. Interestingly, the stress distributions are exponential at the contact zones and they are mainly guided by the particle phase in compression and by the matrix in tension. We also show that the distributions are increasingly broader for a decreasing matrix volume fraction in tension whereas in compression they depend only on the particle stiffness.

DOI: 10.1103/PhysRevE.79.051302 PACS number(s): 45.70.−n, 61.43.−j, 83.80.Fg

The highly inhomogeneous nature of force transmission in granular media is a recurrent research topic that has motivated careful experimental work and numerical simulations for 15 years [1–5]. A basic observation is that the force network involves two mechanically distinct subnetworks [6]: (1) strong forces (or force chains), typically above the mean force, with a decreasing exponential distribution and (2) weak forces with a nonvanishing probability even at vanishingly small forces. These robust features are not only essential to the rheology of granular materials, but appear to be more generally a hallmark of jammed systems [7].

The problem is that this whole body of interesting findings concerns basically *model* granular systems with highly simplified composition and texture. Most granular materials encountered in nature or in industry involve however deformable particles embedded in a solid matrix of variable volume and cohesion with the particles. Well-known examples are sedimentary rocks (sandstones, conglomerates, and breccia), biomaterials such as wheat endosperm (starch granules forming a compact structure bound together by a protein matrix) [8,9], and many geomaterials such as mortars, concrete, and asphalt (aggregates of various sizes glued to each other by a cement paste) [10]. It is not obvious to what extent the well-known characteristics of force transmission established for model granular systems can be applied to this broad class of granular materials with complex microstructure. Does the presence of a particulate backbone suffice to produce the same heterogeneous force distributions as in model granular media? One fundamental issue is how a pore-filling solid matrix affects stress transmission and in which respects it depends on the matrix volume fraction. It is not neither straightforward to generalize the force distributions under compressive loading to the case of tensile loading for a cohesive particle-matrix interface. In a similar vein, the role of particle stiffness and extended contact zones between the particles in stress transmission is not evident.

To deal with these issues, one clearly needs an approach in which the stresses can be resolved at subparticle (and submatrix) scales. Thereby, not only the stresses are obtained in the bulk of the particles and matrix, but also the contact forces can be accessed by coarse graining from the stresses at finer scales. This approach enables us to revisit and validate also the contact force distributions established in the limit of infinitely rigid particles without matrix as in model granular media used, e.g., in discrete element methods (DEM).

In this paper, we propose such a methodology based on a lattice-type discretization of the particles, matrix, and their interface. In this method, to which we refer below as lattice element method (LEM), the elastic deformations of the particles are taken into account not only at their contacts with other particles or with the matrix, as in DEM, but also in their bulk. The matrix is introduced with variable volume in the pores between the particles with its elastic properties and adhesion with the particles. The LEM is numerically efficient enough that samples of a large number of well-resolved particles can be simulated. Our findings are consistent with the idea that the granular backbone is at the origin of stress chains that are evidenced also in the presence of a matrix. By comparing the force distributions in a packing simulated alternatively by LEM and DEM in the limit of low matrix volume fractions, we demonstrate the relevance of both methods. The matrix volume fraction, particle stiffness, and loading affect appreciably the level of force heterogeneity, which is reflected in the width of stress distributions.

The LEM has been extensively used for the statistical mechanics of fracture in disordered media and applied to study the fracture properties of ceramics, concrete [10], and biomaterials such as wheat endosperm [8,9]. The space is discretized as a grid of points (nodes) interconnected by one-dimensional elements (bonds). Each bond can transfer normal force, shear force, and bending moment up to a threshold in force or energy representing the cohesion of the phase or its interface with another phase. Each phase (particle, matrix) and its boundaries are materialized by the bonds sharing the same properties. The samples are deformed by imposing displacements or forces to the nodes belonging to the contour. The total elastic energy of the system is a convex function of node displacements and thus finding the unique equilibrium configuration of the nodes amounts to a minimization problem. Performing this minimization for stepwise loading corresponds to subjecting the system to a

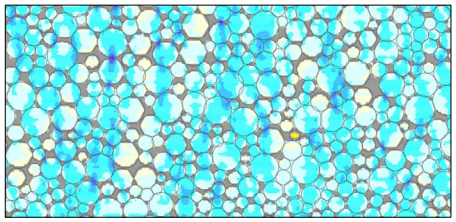

FIG. 1. (Color online) Vertical stress field σ_{yy} represented in color level.

quasistatic deformation process. The method used here can be found in more detail in Ref. [9].

We first focus on the stresses in a packing subjected to vertical compression with free lateral boundaries. The packing is constructed by isotropic compaction of a gaz of disk-like particles by DEM simulations in 2D by setting the friction coefficient between the particles to zero in order to get a dense packing. A rectangular portion of this packing containing about 5000 particles is discretized on a triangular lattice. The solid fraction is $\rho \simeq 0.8$. The particle diameter d varies between d_{min} and $d_{max}=3d_{min}$ with a uniform distribution by volume fractions $[P(d) \propto d^2]$. The matrix is introduced in the form of bridges of variable width depending on the overall matrix volume fraction between neighboring particles distributed homogeneously throughout the system. The elastic properties of each phase are controlled by the linear elastic properties of the bonds. The main elastic parameters that will be considered in this paper are the Hooke constants k^p and k^m of the bonds belonging to the particles and matrix, respectively. The corresponding coarse-grained stiffnesses are $E^p = \sqrt{3}k^p/(2a)$ and $E^m=\sqrt{3}k^m/(2a)$, where a is the bond length, for a regular triangular lattice [9]. The initial state is the reference (unstressed) configuration. Under vertical deformation, the bonds deform and a stress field develops inside the packing. A stress tensor σ^a can be attributed to each node a of the lattice network [9,11]: $\sigma_{ij}^a=\frac{1}{V^a}\Sigma_b r_i^{ab} f_j^{ab}$ where the summation runs over all neighboring nodes j, r_i^{ab} is the i component of the vector joining the node a to the midpoint of the bond ab, and f_j^{ab} is the j component of the bond force.

Figure 1 shows the vertical stress field σ_{yy} for a small vertical compression of a packing with a small matrix volume fraction ρ^m. The node stresses are represented by proportional color levels over the elementary hexagonal cells centered on each node. We observe chains of highly stressed particles and higher concentration at the contact zones between the particles. Note that in this example the deformations are elastic and no bond is damaged. A bond can be damaged if a threshold in force is reached, but this is not of concern in this paper where we assume that all the bonds are active.

In order to compare the LEM simulated packing with DEM simulations of the same packing, for which only contact forces are accessible, we compute the contact forces $\vec{f}$ by summing up the bond forces $\vec{f}^{ab}$ for all bonds ab crossing the contact plane S: $\vec{f}=\Sigma_{ab \in S}\vec{f}^{ab}$. Figure 2 shows the map of normal forces between particles for the LEM packing as well as for the same sample simulated by DEM with adhesion, i.e., by introducing a tensile strength at the contact points between the particles. We observe strikingly similar force chains although the two methods are radically different. The probability density functions (pdf's) of normal and tangential forces from LEM and DEM simulations are shown in Fig. 3. We observe that the two pdf's coincide over nearly the whole range of forces. This agreement between the two methods is all the more interesting that in DEM the particles are assumed to be rigid and the stresses inside the particles are not involved in the calculation of contact forces. The pdf has the well-known features of force distributions in dry granular media The forces below the mean have a nearly uniform distribution whereas larger forces represent a nearly exponential decay: $P_f(f_n) \propto e^{-\beta f_n/\langle f_n \rangle}$. This excellent agreement between the force pdf's with $\beta \simeq 1.35$ may be considered as a validation of DEM simulations in the sense that the contact forces in LEM simulations are calculated from finer scale [2,4,5].

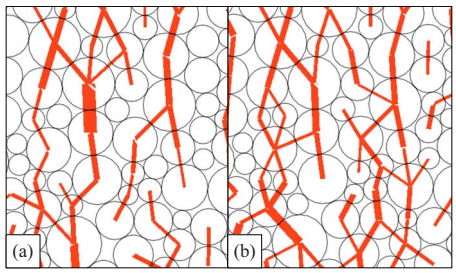

FIG. 2. (Color online) A map of normal forces in a portion of a sample under vertical compression simulated by (a) DEM and (b) LEM. Line thickness is proportional to the normal force.

We now use LEM simulations to analyze the distributions of stress components inside the packing for a $\rho^m=0.01$. This corresponds to thin matrix bridges between the particles. The pdf of the vertical stresses σ_{yy} is displayed in Fig. 4(a) for a packing under vertical compression. Since the sample is un-

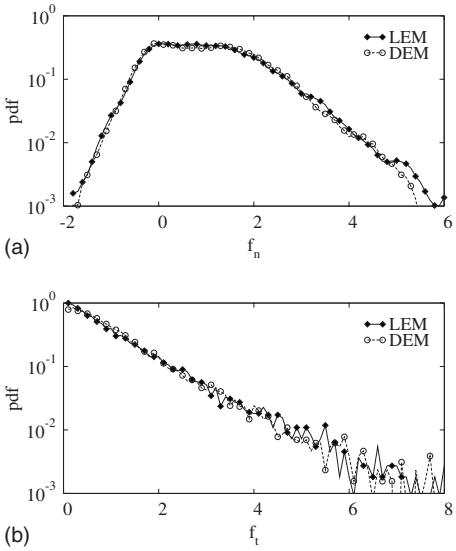

FIG. 3. Probability density function of normal forces (a) and tangential forces (b) in a sample axially compressed by LEM and DEM simulations. The forces are normalized by the mean normal force.

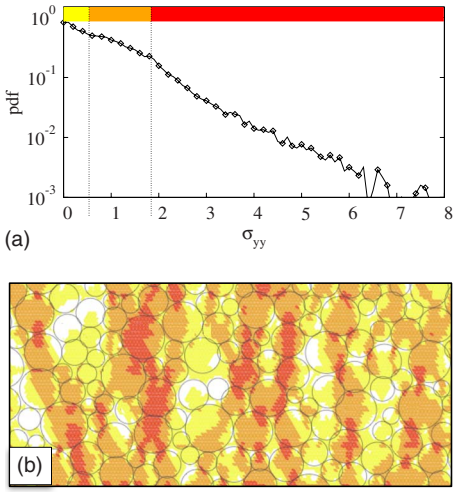

FIG. 4. (Color online) (a) Probability density function of vertical stresses normalized by the average stress in compression. (b) Tricolor map of vertical stresses with weak, intermediate, and strong stresses represented in yellow, orange, and red, respectively.

der axial compression, only 4% of vertical stresses are tensile and are thus not shown in Fig. 4(a). The stress pdf can be split into three parts for weak, intermediate, and strong stresses a map of which is shown in Fig. 4(b). The strong stresses fall off exponentially as contact forces (see Fig. 3), $P_\sigma(\sigma_{yy}) \propto e^{-\beta\sigma_{yy}/\langle\sigma_{yy}\rangle}$ with $\beta \simeq 0.95$, and they mostly concentrate at the contact zones. The weak stresses have nonzero pdf, much the same as weak contact forces, reflecting the arching effect, and they occur mainly inside the unstressed particles or in unstressed parts of the particles. Finally, the intermediate stresses are centered on the mean and are almost totally localized inside the particles.

It is expected that at higher matrix contents the stress is more homogeneously redistributed inside the packing. Figures 5(a) and 5(b) show P_σ for three values of ρ^m in tension and compression for $k^p = 100k^m$. The exponential tail persists both in tension and in compression, but at similar matrix volume fraction, the pdf of strong stresses is broader in compression than in tension. This means that stress redistribution is more homogeneous in tension than in compression.

It is also interesting to observe that the stress pdf is not affected by the matrix volume fraction in compression but it is increasingly broader in tension for decreasing matrix content so that the stresses are more and more concentrated in the bridges between the particles. In tension, the exponent β varies from 1.10 to 2.55 as ρ^m varies from 0.08 to 0.12 whereas in compression we have $\beta \simeq 0.95$ for all ρ^m. As the ρ^m increases, the pdf of intermediate stresses, corresponding mainly to the stresses in the bulk of the particles, becomes peaked on the mean stress.

We now consider the influence of relative stiffness k^p/k^m on stress distributions. Figures 6(a) and 6(b) show the vertical stress pdf's for three values of k^p/k^m in tension and compression for $\rho^m = 0.10$. It is remarkable that in tension the particle stiffness has little influence on the pdf whereas in compression the pdf becomes increasingly broader for an increasing particle stiffness. The respective effects of particle stiffness and matrix volume fraction can be understood by

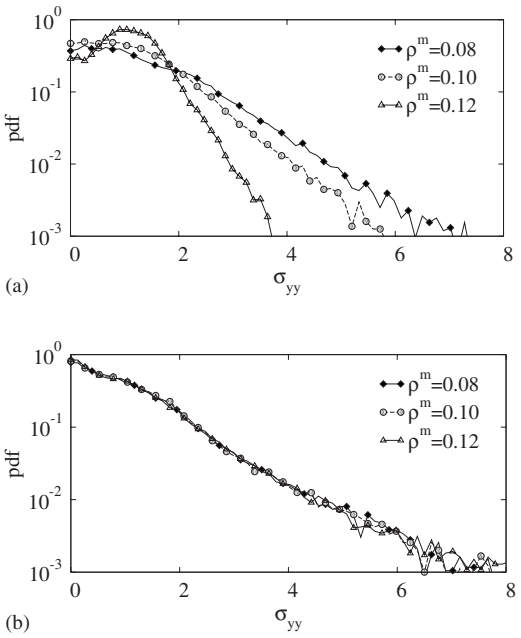

FIG. 5. Probability density functions of normalized vertical stresses for three values of the matrix volume fraction (a) in tension and (b) in compression. For the sake of visibility, there are more data points than symbols.

remarking that, due to the presence of a granular backbone, the stress chains are essentially guided by the cementing matrix in tension and by the particle phase in compression. Therefore, the stress transmission is not affected by the matrix volume fraction in compression and only slightly influenced by particle stiffness in tension.

It is worth mentioning that in our LEM simulations the

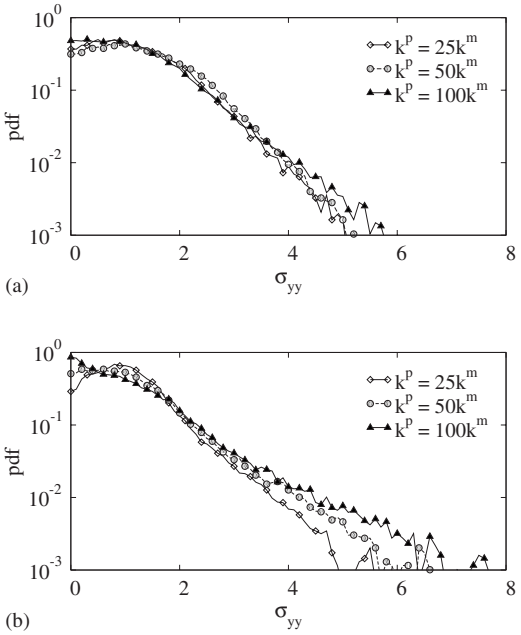

FIG. 6. Probability density functions of normalized vertical stresses for three values of the relative stiffness k^p/k^m (a) in tension and (b) in compression. For the sake of visibility, there are more data points than symbols.

only source of disorder is the particle configuration, the underlying bond network remaining a regular lattice. Hence, the stress distribution and its variability as a function of ρ^m and k^p/k^m are only related to granular disorder. This explains why the stress pdf's are robust and only qualitatively depend on the parameters. In particular, the exponent β of the exponential pdf of strong stresses reflects basically the degree of homogeneity of stress transmission. The trends are similar for the other stress components and for this reason were not shown in this paper.

In short, the LEM approach provides an efficient framework for the investigation of stress fields in more complex granular solids than usually considered model granular media. Using this approach and by integrating subparticle stresses, we arrive at the same contact force distributions as in usual DEM simulations and experiments. Our findings indicate that, irrespective of particle stiffness and matrix volume fraction, the strong stresses are mainly localized at the contact zones between the particles and they have an exponential distribution as strong contact forces. In this way, the well-known properties of force distributions in model granular media can be extended to cemented materials such as concretes, sandstones, and dense particle reinforced composites.

[1] C. Liu, S. R. Nagel, D. A. Schecter, S. N. Coppersmith, S. Majumdar, O. Narayan, and T. A. Witten, Science **269**, 513 (1995).
[2] F. Radjaï, M. Jean, J. J. Moreau, and S. Roux, Phys. Rev. Lett. **77**, 274 (1996).
[3] H. Jaeger and S. Nagel, Rev. Mod. Phys. **68**, 1259 (1996).
[4] D. M. Mueth, H. M. Jaeger, and S. R. Nagel, Phys. Rev. E **57**, 3164 (1998).
[5] T. S. Majmudar and R. P. Behringer, Nature (London) **435**, 1079 (2005).
[6] F. Radjaï, D. E. Wolf, M. Jean, and J. J. Moreau, Phys. Rev. Lett. **80**, 61 (1998).
[7] *Jamming and Rheology*, edited by A. J. Liu and S. R. Nagel (Taylor and Francis, New York, 2001).
[8] V. Topin, F. Radjai, J.-Y. Delenne, A. Sadoudi, and F. Mabille, J. Cereal Sci. **47**, 347 (2008).
[9] V. Topin, J.-Y. Delenne, F. Radjaï, L. Brendel, and F. Mabille, Eur. Phys. J. E **23**, 413 (2007).
[10] E. Schlangen and E. J. Garboczi, Eng. Fract. Mech. **57**, 319 (1997).
[11] J. J. Moreau, in *Friction, Arching, Contact Dynamics*, edited by D. E. Wolf and P. Grassberger (World Scientific, Singapore, 1997), pp. 233–247.